

Measurement of the Extent of Reaction of an Epoxy–Cycloaliphatic Amine System and Influence of the Extent of Reaction on Its Dynamic and Static Mechanical Properties

CATHERINE JORDAN, JOCELYNE GALY,* and JEAN-PIERRE PASCAULT

Laboratoire des Matériaux Macromoléculaires (URA 507), INSA de Lyon, 20, Avenue Albert Einstein, 69621 Villeurbanne, Cedex, France

SYNOPSIS

An investigation was carried out into the effect of the extent of reaction on the mechanical properties, in a mixture of an epoxy prepolymer and a cycloaliphatic diamine, above the gel point. First, the most adequate technique to approach the extent of reaction was chosen between differential scanning calorimetry, Fourier transformation infrared, and size exclusion chromatography. It was found that the differential scanning calorimetry gave a good estimate of the extent of reaction, measuring the glass transition temperature and using a modified DiBenedetto equation. Dynamic mechanical properties and static mechanical properties are shown to be highly dependent upon the extent of reaction. The β relaxation was found to be responsible for the fracture properties at room temperature through the changes in extent of reaction. © 1992 John Wiley & Sons, Inc.

INTRODUCTION

In the last decade, a considerable amount of research has been done on the relationship between structure and physicochemical properties of epoxy networks. It is well known that in the final epoxy network structure the physical and mechanical properties directly depend upon the chemical structure and cure reactions.

Varying the matrix structure is generally proceeded by controlling the crosslink density or the average molecular weight between crosslinks, M_c . The use of different average molecular weight of the epoxy prepolymer, M_E , is the most common way^{1,2} to vary the crosslink density. It introduces a large distribution of the molecular weight between crosslinks. The studies show that the glass transition temperature decreases with increasing M_E or increasing M_c . Another method consists of adding a third monomer, as well as a difunctional monoamine with a structure similar to the tetrafunctional di-

amine. The amine compounds are supposed to have the same reactivity so that the monoamine acts as a chain extender. This technique has been used by many authors.³⁻⁵ The rubbery modulus has been shown to decrease with increasing the amount of monoamine or M_c . The crosslink density can also be varied by changing the stoichiometric ratio hydrogen-to-epoxy, a/e .⁵⁻⁹ This technique introduces dangling chains with unreacted functions. It was found that M_c reaches its minimum for a stoichiometric ratio equal to 1, whereas T_g is maximum.

Little attention has been paid to the level of epoxy networks properties as a function of the degree of cure.¹⁰ The cure schedule or cure time is varied, leading to "opened" networks, with dangling chains or unreacted monomers and sol-gel fractions, compared to other methods where the networks are "closed." Noordam et al.¹⁰ studied the influence of the extent of reaction on many mechanical properties on a batch of epoxy amine networks based upon different DGEBA prepolymers and diamines. Very low crosslinked networks near the gel point showed poor mechanical properties. On the other hand, stiffness and impact behavior had an optimum at 80% of epoxy conversion and decreased with higher extents of reaction.

* To whom correspondence should be addressed.

The majority of methods used for assessing the extent of reaction are very sensitive up to the gelation (the early stages of crosslinking) but fail in the later stages: equilibrium swelling, sol-gel analysis, heat distortion test, surface hardness, water absorption, resistivity methods, dielectric studies, dilatometric methods, infrared analysis, and differential scanning calorimetry (DSC) (measurements of the residual heat of reaction). Noordam et al.¹⁰ used attenuated total reflectance Fourier transform infrared (FTIR) spectroscopy and theoretical calculation according to Flory,¹¹ Stockmayer,¹² and Carothers.¹³ According to Noordam et al.,¹⁰ a good agreement between the calculated and observed values was obtained with the Flory¹¹ and Stockmayer¹² statistic approach in the case of low epoxy conversion from 50 to 70%. Above 70%, the Carothers¹³ approach seemed to better fit the experimental data (even if it is well known that the Carothers approach is not correct). However, for high extents of reaction none of these theories could give a good estimate.

The aim of this work is to analyze the influence of the extent of reaction, x , above the gel point of an epoxy/amine system on the static and dynamic mechanical properties. We will investigate another way to use DSC thermograms, referring to Pascault and Williams,¹⁴ who analyzed different equations that have been proposed to fit experimental data T_g vs. x . The best technique to determine x when it reaches the maximum value of conversion, x_{max} , will be discussed. Mechanical properties such as stiffness, toughness, yield behavior, and viscoelastic properties were tested as a function of the extent of reaction. We tried to establish a structure-property relationship of the various networks besides the complexity of the unclosed networks with dangling chains contributions.

EXPERIMENTAL

Materials

The epoxy prepolymer used in this study was almost pure diglycidyl ether of bisphenol-A (DGEBA): DER 332 from Dow Chemical, with an equivalent weight of epoxy groups equal to 174 g/eq. The curing agent was 4,4'-diamino-3,3'-dimethyldicyclohexylmethane (3DCM, Laromin C 260, from BASF), with a molecular weight of 238 g/mol. Figure 1 shows the structural formulae of both monomers. The reactants were used as received, with a stoichiometric ratio a/e of 1. The formulation is 100 g DGEBA for 34.5 g 3DCM.

Processing

The epoxy prepolymer and the comonomer were mechanically stirred under vacuum at room temperature for one half hour. The mixture was then poured into a $180 \times 180 \times 6$ mm³ dimension mold. Different cure schedules were performed to obtain two kinds of networks. Four precure stages, based upon a time-temperature-transformation diagram previously established by Verchère et al.,¹⁵ led to the synthesis of partially reacted networks. Some of these samples were postcured at a temperature $T_2 = 190^\circ\text{C}$.¹⁵ Table I summarizes the cure schedules chosen for the study.

Characterization of the Epoxy Networks: Epoxy Conversion

A Mettler TA 3000 DSC was used to measure the glass transition temperature, T_g (onset value), and the changes in isobaric heat capacity through the

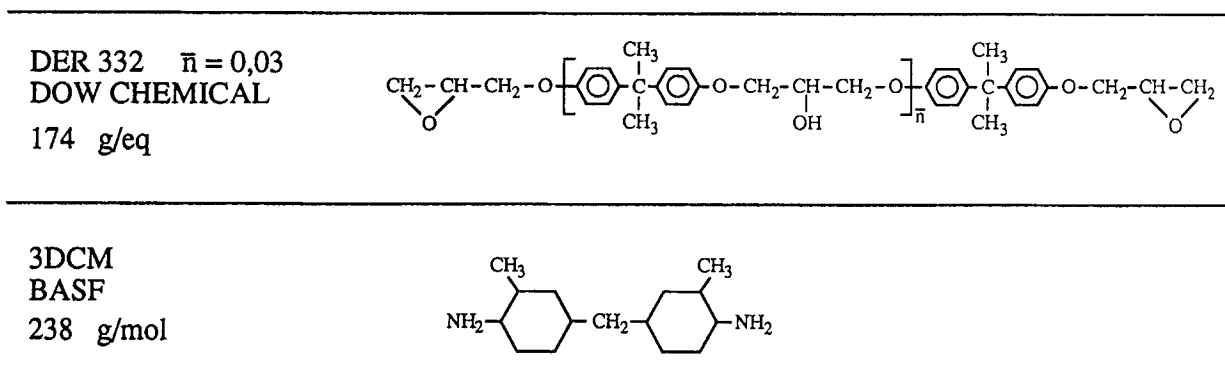


Figure 1 Molecular structure of the epoxy prepolymer and diamine used for the synthesis of the epoxy networks.

Table I Influence of Cure Schedules on the Glass Transition Temperature, Extent of Reaction, and Volumetric Mass of DGEBA–3DCM Networks

Cure Schedule			% Extent of Reaction					ρ (g cm ⁻³)
T_1/T_2 (°C)	t_1/t_2 [(min)/(h)]	T_g (°C)	x_{SEC}	x_{IR}	x_{th}^{a}	x_{th}^{b}	x_{th}^{c}	
50	300	74	63	52	75	74	72	
75	120	88	77	74	80	78	77	1.137
100	80	116	86	87	87	86	84	1.134
120	75	135		90	91	90	88	1.132
140	60	142	93	92	93	92	89	1.129
75/190	120/14	183			100	99.4	96	1.131
100/190	80/14	183			100	99.4	96	1.131
120/190	75/14	183			100	99.4	96	1.132
140/190	60/14	183			100	99.4	96	1.130

^{abc} Comparison of different techniques to measure conversion, x , and x_{th} by DiBenedetto, Hale, and Oleinik, respectively (see text).

glass transition temperature, ΔC_p , of the different samples at 10°C/min heating rate under argon atmosphere.

The extent of reaction is commonly deduced from DSC thermograms by calculating the residual heat of reaction ΔH_R :

$$x = 1 - \frac{\Delta H_R}{\Delta H_0} \quad (1)$$

where ΔH_0 is the total heat evolved by the epoxy-amine reaction. It has been proved that for the DGEBA–3DCM system the residual heat of reaction is hardly detectable for high extents of reaction (above 90%), whereas the glass transition temperature still increases, showing the extent of reaction is not at its maximum value.^{15,16}

Using the original DiBenedetto theoretical equation, we can evaluate the extent of reaction (x) of the thermosets. x depends upon T_{g0} and $T_{g\infty}$, the glass transition temperature of the unreacted mixture ($x = 0$) and the glass transition temperature of the fully reacted network ($x = 1$), respectively.

$$\frac{(T_g - T_{g0})}{(T_{g\infty} - T_{g0})} = \frac{\lambda x}{1 - (1 - \lambda)x} \quad (2)$$

The adjustable parameter λ can be evaluated two different ways:

1. From an extension of the Couchman equation,¹⁷ Pascault and Williams¹⁴ showed that λ is the ratio $\Delta C_{p\infty}/\Delta C_{p0}$ where $\Delta C_{p\infty}$ and

ΔC_{p0} are, respectively, the isobaric heat capacities of the fully reacted network and of the initial unreacted mixture.

2. From the location of $_{\text{gel}}T_g$, the particular temperature at which gelation and vitrification take place simultaneously. If x_{gel} , the extent of reaction at this point, is equal to 0.6 and assuming the validity of eq. (2) we have

$$\lambda = \frac{2({}_{\text{gel}}T_g - T_{g0})}{3(T_{g\infty} - T_{g0})} \quad (3)$$

The main drawback of this equation is the uncertainty in the determination of $T_{g\infty}$ and particularly $\Delta C_{p\infty}$. As a matter of fact, Oleinik¹⁸ showed that theoretically the maximum extent of reaction that can be expected in an epoxy-amine system is $x = 0.95$ – 0.96 : The unreacted epoxy or amino groups are spatially separated from each other and cannot meet and react due to the high connectivity of the network. Thus, the infinite properties of the network cannot be determined by the experiment. We'll discuss later how one can dispense with $T_{g\infty}$ and $\Delta C_{p\infty}$.

Size exclusion chromatography (SEC) was employed to estimate the extent of reaction in epoxy functions in the postgel stage. The amount of solubles in the networks were first collected by Soxhlet extraction in boiling tetrahydrofuran solvent on always the same mass of sample, even after gelation. The unknown concentration of the solution, in epoxy functions, was calculated, following the height

of DGEBA peak, assuming that the epoxy functions are equally reactive and that there is no substitution effect¹⁹:

$$(1 - x)^2 = \frac{h_t}{h_0} \quad (4)$$

This is the simultaneous probability that both epoxy groups remain unreacted on the same molecule, and h_t/h_0 is the ratio of the actual height of the peak with respect to the initial one. It is necessary to emphasize that the assumption of equal reactivity of the epoxy functions has been measured experimentally with the help of the SEC only up to the gelation point. However, statistical predictions after gelation are correct with the absence of a substitution effect.²⁰ At high extents of reaction, topological limitations produce an effect of nonequal reactivity, and if we assume, as Oleinik,¹⁸ that due to steric hindrance $x_{\max} = 0.96$ then it is certain that for high conversions the epoxy functions do not have equal reactivity.

Infrared analyses were performed on a Nicolet MX-1 FTIR spectrometer with KBr pellets containing the finely ground material. The phenyl group band (1180 cm^{-1}) was used as a reference since it is assumed to be unmodified during the reaction.²¹ The disappearance of the epoxy functions was followed with the height of the epoxy band (915 cm^{-1}) with respect to the phenyl band height.

Specific weight measurements proceeded for all samples with Archimedes' principle in water at 25°C .

Characterization of the Epoxy Networks: Mechanical Measurements

Dynamic mechanical measurements were performed with a Rheometrics RDA 700 apparatus in torsion mode at 11 Hz. Storage shear modulus G' , loss shear modulus G'' , and loss factor $\tan\delta$ were recorded during a temperature ramp from -150 to $+110^\circ\text{C}$ for partially crosslinked networks and from -150 to $+250^\circ\text{C}$ for fully reacted networks. A special study was carried out for fully crosslinked networks in the glass transition region ($T_g - 30^\circ\text{C}$ to $T_g + 30^\circ\text{C}$). The time (or frequency)–temperature superposition principle [Williams–Landel–Ferry (WLF) equation] was used to determine the viscoelastic coefficients C_1 and C_2 , which are related to the free volume characteristics on the molecular scale. G' , G'' , and $\tan\delta$ were measured as a function of frequency (from 10^{-1} – $10^{+2} \text{ rad s}^{-1}$ with five angular frequencies per decade). In the glass transition region, the temper-

ature dependence of the horizontal shift factor, a_T , obeys the WLF equation²²:

$$\log a_T = \log \frac{f}{f_0} = -\frac{C_1(T - T_0)}{C_2 + T - T_0} \quad (5)$$

where f_0 and f are the frequencies of the motions, respectively, at the reference temperature T_0 and at the temperature T . We refer to Gérard et al.²³ to determine the viscoelastic parameters.

C_1 and C_2 , corresponding to the reference temperature T_0 , are related to C_1^g and C_2^g , associated to T_g by the relationships

$$C_1^g C_2^g = C_1 C_2 \quad \text{and} \quad T_g(1 \text{ Hz}) - C_2^g = T_0 - C_2 \quad (6)$$

The reference temperature $T_g(1 \text{ Hz})$ is defined as the temperature at which G'' goes through a maximum when the frequency is 1 Hz.

C_1^g and C_2^g can be related to quantities on the molecular scale by assuming the validity of two relationships associated with the free volume concept:

1. The Doolittle equation,²⁴ which correlates the viscosity η to the free volume v_f

$$\ln \eta = \ln A + B \left(\frac{v - v_f}{v} \right) \quad (7)$$

where A and B are empirical constants depending upon the polymer structure.

2. The linear variation in fractional free volume as a function of temperature:

$$f_T = f_g + \alpha_f [T - T_g(1 \text{ Hz})] \quad (8)$$

Combination of eqs. (7) and (8) finally yields the relationships:

$$C_1^g = \frac{B}{2, 3 f_g} \quad \text{and} \quad C_2^g = \frac{f_g}{\alpha_f} \quad (9)$$

Tensile tests were made with an Adamel Lhomargy (DY25) machine at room temperature with a strain rate of $6.6 \cdot 10^{-4} \text{ s}^{-1}$. Specimen elongations were monitored using an extensometer (Adamel Lhomargy EX10). Young's moduli in the vitreous state E_v were calculated from the initial part of the stress–strain curves.

Compression tests were made with the same machine as used for the tensile tests, using parallel-epipedic samples ($20 \times 12 \times 6 \text{ mm}^3$) deformed in a compression rig at a strain rate of $8.3 \cdot 10^{-4} \text{ s}^{-1}$. The yield stress σ_y and the yield strain ϵ_y were determined.

Single-edge notched (SEN) specimens were used in three point-bending modes (span to length = 48 mm). Specimen thickness, w , was about 12 mm and width, l , about 6 mm. Cracks of various lengths were tailored with a saw and the crack tip was achieved with a razor blade at room temperature. The radius of the tip was about 1 μm , and its length is a . Fracture toughness was calculated using the formula

$$K_{Ic} = \frac{\sigma_c (\pi a)^{1/2}}{f(a/w)} \quad (10)$$

where σ_y is the critical stress for crack propagation and $f(a/w)$ a form factor previously described.²⁵ The fracture energy G_{Ic} in plane strain condition is given by

$$G_{Ic} = \frac{K_{Ic}^2 (1 - \nu^2)}{E_v} \quad (11)$$

where ν is the Poisson ratio and E_v is Young's modulus.

RESULTS AND DISCUSSION

Glass Transition Temperature and Extent of Reaction

The DSC measurements made on the networks without a postcure stage show that the glass tran-

sition temperature increases with increasing cure temperature (see Table I). When the networks are postcured ($T_2 = 190^\circ\text{C}$, $t_2 = 14$ h), T_g reaches a maximum that does not vary significantly with the temperature of the first stage of cure, $T_{g\infty} = 183 \pm 3^\circ\text{C}$.

We now investigate the equation that could better fit the experimental data of x vs. T_g .

1. First, we assume that the postcured networks have an extent of reaction of 1. Thus, $T_{g\text{max}} = T_{g\infty} = 183^\circ\text{C}$. T_{g0} is taken equal to -32°C , $\Delta C_{p\infty} = 0.19 \text{ J g}^{-1} \text{ k}^{-1}$, and $\Delta C_{p0} = 0.59 \text{ J g}^{-1} \text{ k}^{-1}$. These are the mean values of 10 experiments. The standard deviation is 3°C for $T_{g\infty}$, 1°C for T_{g0} , and $0.02 \text{ J g}^{-1} \text{ k}^{-1}$ for both heat capacities. None of the measured samples showed any physical aging, which would consistently influence ΔC_p measurements. The DiBenedetto curve $x = f(T_g)$ is shown in Figure 2 (pointed line). The extents of reaction found with the SEC, x_{SEC} , and FTIR, x_{IR} , techniques are reported in the same figure.

Verchère's DSC measurements,¹⁵ obtained from eq. (1), are reported in Figure 2 (\cdot). A good agreement with the theoretical curve is observed. The experimental value of ${}_{\text{gel}}T_g = 48^\circ\text{C}$ largely differs from the ${}_{\text{gel}}T_g = 37^\circ\text{C}$

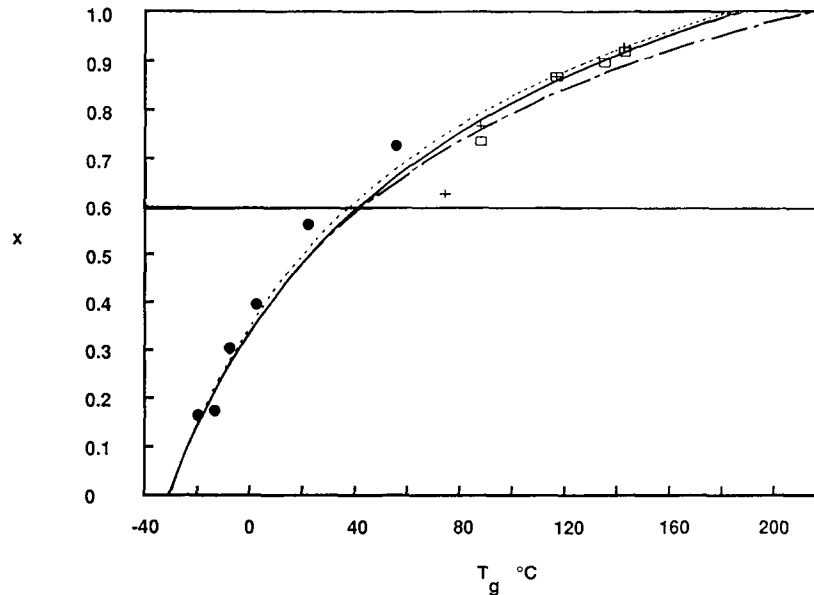


Figure 2 Extent of reaction as a function of the glass transition temperature. (. . .), $\lambda = \Delta C_{p\infty} / \Delta C_{p0} = 0.32$, $T_{g\infty} = 183^\circ\text{C}$, $x = 1$; (—), $\lambda = \Delta C_{pM} / \Delta C_{p0} = 0.39$, $T_{gM} = 142^\circ\text{C}$, $x_M = 0.92$; (---), $\lambda = \Delta C_{pM} / \Delta C_{p0} = 0.32$, $T_{gM} = 183^\circ\text{C}$, $x_M = 0.96$; (+), x_{SEC} ; (\square), x_{IR} ; (\cdot), x_{DSC} from eq. 1 (Verchère).

given by the curve for $x = 0.6$. The theoretical curve roughly fits the experimental extents of reaction above 0.8. One can note that a small increase in extent of reaction leads to a significant increase in T_g due to the slope of the DiBenedetto curve in the high T_g region. This means that the method is able to detect a small variation in the extent of reaction, as soon as the T_g measurement is precise at the end of the reaction, when other methods fail. As a matter of fact, the FTIR analysis was unable to give any information about the amount of epoxy functions left in the 140/190 network.

- It is convenient to think that the postcured networks reached a maximum glass transition temperature, which is $T_{g\infty}$. It is possible, however, that this glass transition temperature should only be considered a maximum $T_{g\max}$, corresponding to an extent of reaction x_{\max} unknown. Oleinik¹⁸ suggested that for an epoxy-amine system x_{\max} should be equal to 0.95–0.96. Hale et al.¹⁶ found, for their epoxy-novolac system, an optimum conversion of 0.85. They explained this low value by more severe topological limitations because their system had a much higher functionality than an amine-epoxy system. To estimate $T_{g\infty}$, they suggested to restate eq. (2) as

$$\frac{(T_g - T_{g0})}{(T_{gM} - T_{g0})} = \frac{\lambda' x'}{1 - (1 - \lambda') x'} \quad (12)$$

where T_{gM} is the glass transition temperature of a network whose extent of reaction is perfectly known and close to 1. x' is the ratio x/x_M , where x_M is the extent of reaction of the network showing $T_g = T_{gM}$. $\lambda' = \Delta C_{pM} / \Delta C_{p0}$. ΔC_{pM} is the changes in heat capacity through the glass transition of the T_{gM} network.

We apply eq. (12) to our system to determine whether undetectable epoxy functions remain unreacted in the postcured samples, which could explain the shift in $_{\text{gel}}T_g$ compared to the experimental value. To apply eq. (12), we take the experimental point, $T_{gM} = 142^\circ\text{C}$, $x_M = 0.92$, $\Delta C_{pM} = 0.23 \text{ J g}^{-1} \text{ K}^{-1}$. This new theoretical curve gave the theoretical values $_{\text{gel}}T_g = 41^\circ\text{C}$ and $T_{g\infty} = 187^\circ\text{C}$ (plain line in Fig. 2). According to eq. (12), the postcured networks should have an extent of reaction of 0.99. This seems to be consistent with the fact that none of the methods

tested could detect any unreacted epoxy functions.

- It is also possible to consider the DiBenedetto curve constructed with the theoretical value of the maximum extent of reaction calculated by Oleinik¹⁸: $x = 0.96$ for $T_{g\max} = 183^\circ\text{C}$. In this case, $_{\text{gel}}T_g = 43^\circ\text{C}$ whereas $T_{g\infty} = 214^\circ\text{C}$ (broken line in Fig. 2). It seems that even if the theoretical $_{\text{gel}}T_g$ value is closer to the experimental value it is not reasonable to take this latter curve into account. As a matter of fact, the FTIR method would be able to detect 4% of unreacted epoxy functions in the postcured samples and this is not the case. The extraction of the postcured samples showed that no DGEBA prepolymer molecules could be detected by SEC. The very low quantity of extracted sol fraction was analyzed by FTIR but no reactive epoxy functions could be observed. The presence of CH groups could be attributed to a degradation of the network after too long a stay in hot solvent. Statistical calculations predict that if x is reaching 1 the sol fraction should be almost pure DGEBA. Consequently, the absence of DGEBA in the solution attests that $x \sim 1$.

As a first conclusion, it seems that the approach of the DiBenedetto curve developed by Pascault and Williams¹⁴ in the form used by Hale et al.¹⁶ fits better the experimental data. It is thus this equation that is kept for the calculation of x_{th} . On the other hand, one should keep in mind that it is not necessary to use any adjustable parameters nor make statistical calculations assuming a particular model for the network build-up. However, the goodness of fit is in part due to the fact that the curve is forced to pass through T_{gM} . This equation will be of great interest for the following work because it will give the extent of reaction of any sample by a very classical T_g measurement, especially for high conversions when other methods are inaccurate.

Specific Mass of the Epoxy Networks

The specific mass of the samples is plotted as a function of the extent of reaction (see Fig. 3). It slightly decreases with decreasing the molecular weight between crosslinks. Enns and Gillham,²⁶ using a rigid bisphenol-A-based prepolymer, reported the same variation, whereas Misra et al.¹ verified the opposite on a batch of amine-cured epoxies.

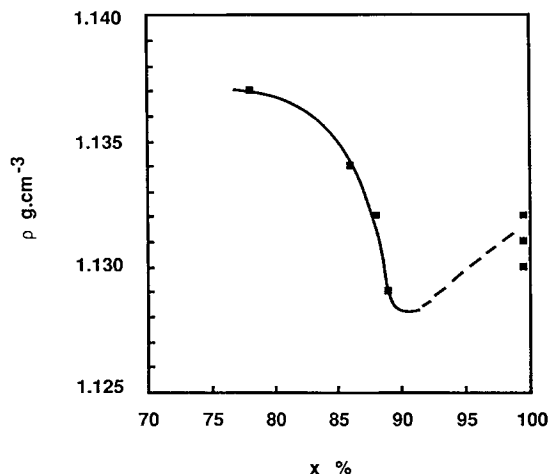


Figure 3 Specific mass as a function of the extent of reaction: DGEBA-3DCM network.

Gupta²⁷ in a large review of the literature emphasized the diversity of behaviors concerning the specific mass dependence upon the crosslink density. The specific mass is greatly dependent upon the chain stiffness of the amine comonomer and of the prepolymer. Bellenger et al.²⁸ pointed out the fact that a specific mass decrease can be attributed to changes of van der Waals volume related to the epoxy-amine addition. Won et al.²⁹ showed that the specific mass variations at the second decimal level can mainly be attributed to the fraction of heavy heteroatoms (essentially oxygen). It is constant in this study and we can attribute the changes of the third decimal level to the variation in crosslink density. It is not clear that the very small variation in specific mass should induce a variation in vitrous modulus. Won et al.³⁰ established a good correlation between the room temperature tensile modulus and the crosslink density but the networks based upon epoxy-diamine-monoamine showed no specific behavior of the specific mass with tensile modulus. The variations of the specific mass of the DGEBA-3DCM networks with Young's modulus will be discussed later.

Viscoelastic Properties of the Polyepoxy Networks

1. Partially cured networks were studied at low temperatures, where samples do not undergo further curing. In Figure 4, loss factor ($\tan\delta$) is recorded vs. temperature at a frequency of 11 Hz. The $\tan\delta$ vs. temperature curves pass through a maximum near -50°C (β peak). This mechanical relaxation is associated with

two kinds of molecular segments. At high temperatures ($T > -50^\circ\text{C}$), the hydroxyether moieties relax, whereas at lower temperatures ($T < -50^\circ\text{C}$) the motions of diphenylpropane groups supply their contribution to the β relaxation.^{31,32}

Hydroxyether groups concentration increases upon curing, as a result of the epoxy-amine reaction, leading to the transformation of the shape of the β peak. The peculiar structure of the partially cured networks, composed of crosslinked segments and dangling chains of various sizes, provides a large variety of behaviors of the diphenylpropane and hydroxyether units during the relaxation. Charlesworth³ showed that the specific loss is more dependent upon the neighboring group interactions than on the crosslink density.

A special point appears at -90°C where all the curves pass through. This noteworthy point will be considered as the beginning of the β relaxation whereas the end of the β peak occurs at $+10^\circ\text{C}$. In this range of temperatures, the decrease in G' is of very low magnitude but can be displayed. In Figure 5, the ratio $(G'_{-90^\circ\text{C}} - G'_{+10^\circ\text{C}})/G'_{-90^\circ\text{C}}$, representative of the area below the β peak, is plotted vs. the extent of reaction (Table II). We do not take into account the absolute values of moduli because of the errors introduced by the compliance of the instrument, which depends upon the sample dimensions and the strain imposed. The former ratio increases with increasing x . The storage modulus at room temperature is dependent upon the magnitude of the β relaxation, which conditions the decrease in modulus from low temperatures to room temperature. Won et al.³⁰ found the same variation in tensile vitrous modulus with the crosslink density for copolymers and terpolymers polyepoxy systems. They showed that this phenomenon, which they called antiplasticization phenomenon, is correlated to the effect of crosslinks on the local mobility. Internal antiplasticization phenomenon is the term used in the case of a decrease in modulus associated with an increase in T_g . Arridge and Speake³³ observed the equivalent phenomenon on a DGEBA-triethylene tetramine with increasing the degree of cure. They also attributed the decrease in modulus on the high-temperature side to changes of segment mobility. Our results are

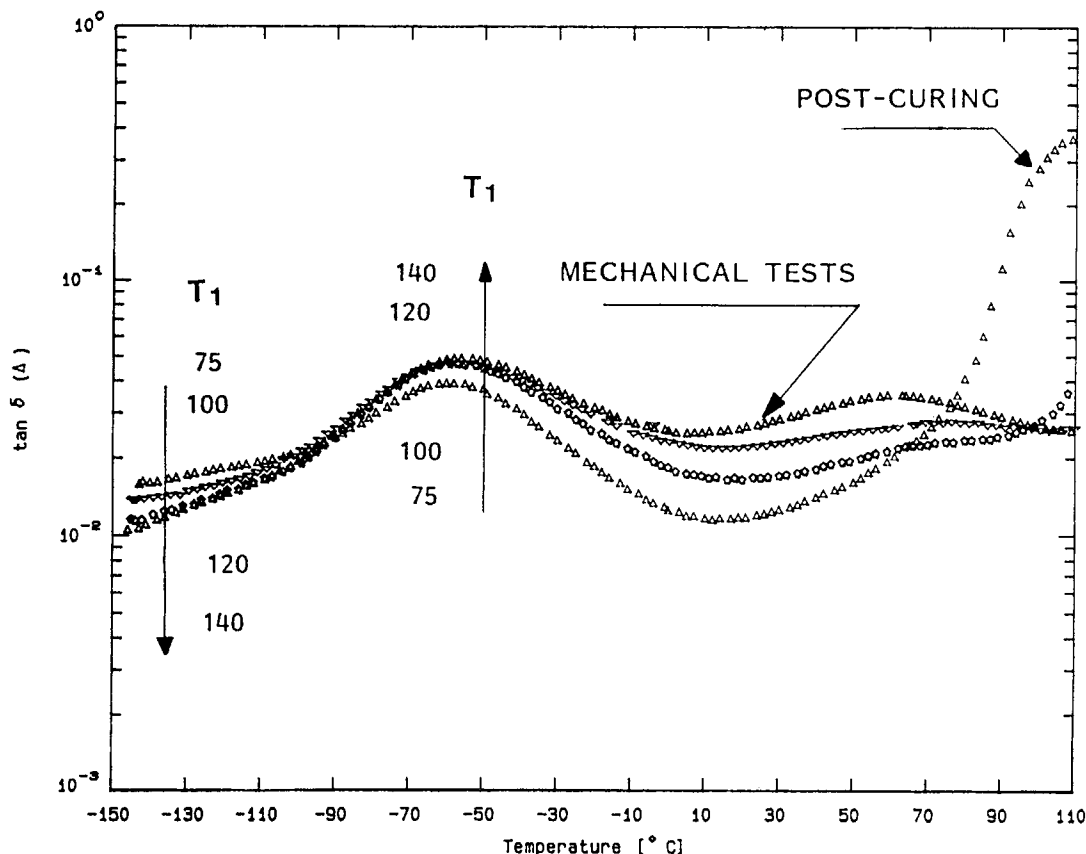


Figure 4 Dynamic mechanical spectrum of the β relaxation for the DGEBA-3DCM networks cured at 75, 100, 120, and 140°C. Loss factor $\tan\delta$ at 11 Hz.

in good agreement with the observations depicted in the literature.

2. The fully reacted networks all show the same viscoelastic behavior over a large range of

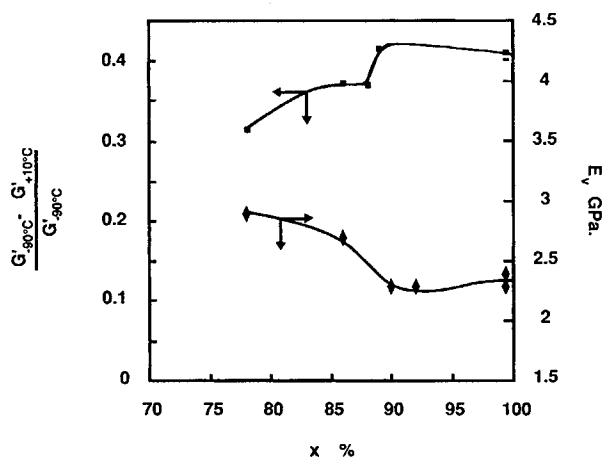


Figure 5 Magnitude of the β relaxation represented by the modulus ratio below and above the transition as a function of the extent of reaction. Young's modulus vs. x .

temperatures (from -150°C to 250°C). Three relaxations are observed: the β relaxation already cited; the ω relaxation, probably corresponding to the cyclohexyl moieties mobility, at about 75°C ; and the main relaxation α related to the glass transition temperature, which appears at 208°C (Fig. 6). The four postcured matrices show the same viscoelastic behavior except in the 150°C region, where the 75/190 and the 100/190 networks have an unexpected shoulder appearing on the main relaxation α . Physical aging is not responsible for these characteristics because the samples have been heated and quenched before the mechanical analysis. More work is needed to elucidate this behavior.

3. The methodology detailed in the experimental section for the determination of the viscoelastic parameters C_1^{β} and C_2^{β} was successfully applied to all the experiment data. Table III summarizes the calculated characteristics C_1^{β} , C_2^{β} , α_f , and f_g .

Table II Storage Moduli as a Function of Temperature Below and Above the β Relaxation Associated with the Fracture Results

Network	$G'_{-90^\circ\text{C}}$ (GPa)	$G'_{+10^\circ\text{C}}$ (GPa)	$\frac{G'_{-90^\circ\text{C}} - G'_{+10^\circ\text{C}}}{(G'_{-90^\circ\text{C}})}$	K_{Ic} (MPa, m ^{1/2})
75	1.707	1.173	0.313	0.98
100	1.937	1.215	0.373	0.8
120	1.795	1.132	0.369	0.7
140	2.040	1.195	0.414	0.71
75/190	2.173	1.297	0.403	0.78
100/190	2.066	1.220	0.409	0.73
120/190	1.458	0.870	0.403	0.75
140/190	2.206	1.313	0.405	0.75

C_1^g and C_2^g are considered constant within the uncertainty of the determination. C_1^g is equal to 10.7, with a variation of 4% between the lowest and highest values. C_2^g is equal to 40.6°C, with a variation of 7%. C_1^g and C_2^g are systematically smaller than the universal values reported by Ferry³⁴: $C_1^g = 17.4$ and

$C_2^g = 51.6^\circ\text{C}$. This seems to be in reasonable agreement with the few values available in the literature for cured epoxy networks (see Table III). Perret³⁵ found C_1^g values between 10.5 and 13 for the DGEBA-diamine diphenyl methane (DDM) matrix with hydrogen to epoxy ratios lower or equal to 1. Gérard

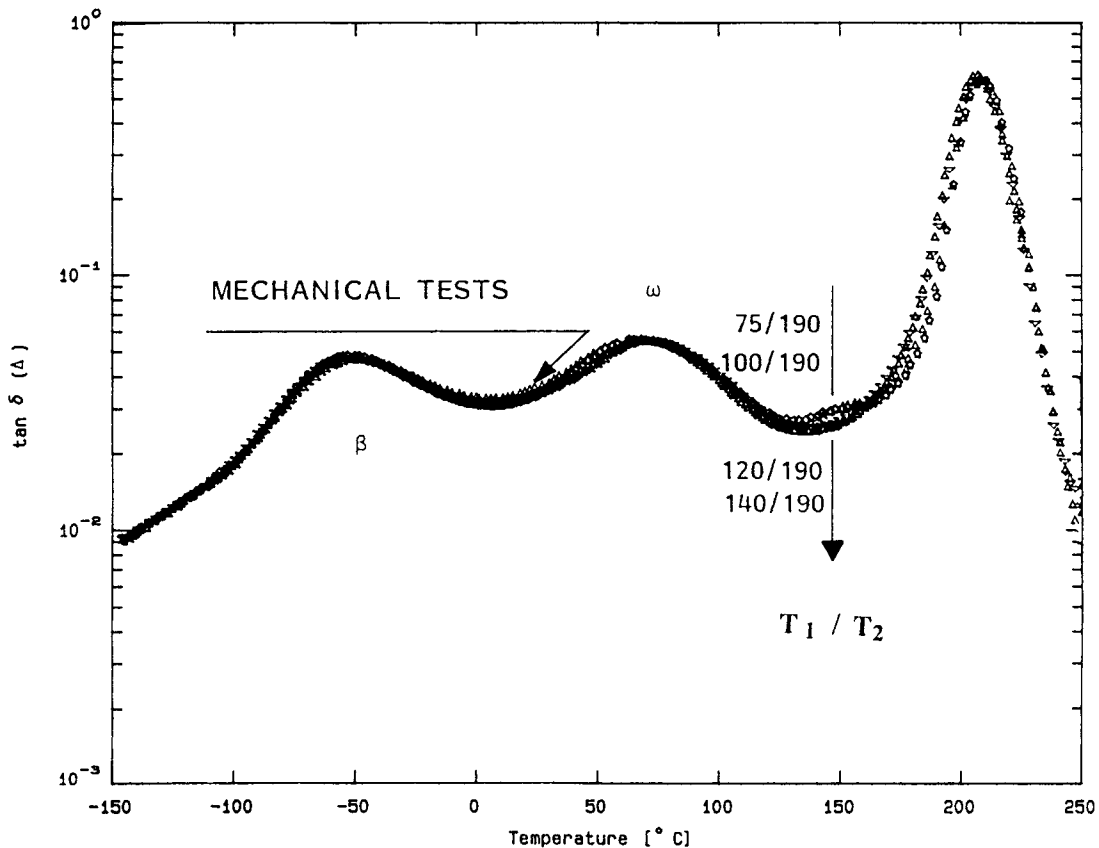


Figure 6 Dynamic mechanical spectrum of the 75/190, 100/190, 120/190, and 140/190 networks. Loss factor $\tan\delta$ at 11 Hz.

Table III Computed Viscoelastic Characteristics of the DGEBA–3DCM Networks

Network	C_1^g	C_2^g (°C)	$C_1^g C_2^g$ (°C)	$10^2 f_g/B$	$10^3 a_f/B$
75/190	10.9	39.3	428	3.98	1.015
100/190	10.7	40.4	432	4.06	1.005
120/190	10.8	41.9	452	4.02	0.961
140/190	10.5	40.7	427	4.14	1.017

et al.²³ and Won et al.⁵ found C_1^g values between 9.2 and 12.5 for polyepoxy networks with different diamines or stoichiometric ratios or for terpolymers containing various amounts of monoamine. The observed values are close enough, with respect to the uncertainty of the determination, to conclude the similarity of the four networks. Williams et al.²² reported that the empirical constant B that allows to compute f_g , the free volume fraction at T_g , and the thermal expansion coefficient, α_f , is not equal to 1²⁴ but varies from 0.6–1.2. Without entering into this discussion, we considered α_f/B and f_g/B only. The values of f_g/B are in good agreement with Gérard et al.'s²³ results, but α_f/B seems lower, corresponding to a higher rigidity of the chains. However, it is not possible in our case to distinguish one network from another. The first stage of cure does not influence the viscoelastic properties and the free volume behavior since the postcure step homogenizes all the samples. This is possible in the case of DGEBA–3DCM networks because of the unique epoxy/amine reaction leading to the same networks disregarding the temperature

schedule. But, it has not been possible to attribute the shoulder appearing on the 75/190 and 100/190 networks to any chemical or physical parameter.

Influence of the Extent of Reaction on the Static Mechanical Properties

The mechanical properties such as Young's modulus E_v , the critical stress intensity factor K_{Ic} , the critical strain energy release rate G_{Ic} , the yield stress σ_y , and the yield strain ϵ_y are reported in Table IV. Very low crosslinked networks ($T_1 = 50^\circ\text{C}$, $x = 0.75$) were particularly brittle and none of the properties could be measured.

Young's modulus E_v is plotted in Figure 5. E_v decreases as the extent of reaction increases up to 90%. The values are slightly higher for further reaction. The postcured samples are considered equivalent since the modulus values prevent from distinguishing one sample from another. These results are surprising since one should expect a better stiffness for a higher density of covalent bonds in larger crosslinked matrix. Noordam et al.¹⁰ observed the same variation in flexural modulus, flexural strength, and impact resistance with conversion. According to Noordam et al.,¹⁰ who worked on DGEBA–diamine systems (including the DGEBA–3DCM system), the decrease in mechanical properties can be attributed to an increase in free volume: Upon cooling, a matrix with a high crosslink density will have a more restricted molecular mobility and thus be less able to closely pack in the glassy state. This implies an increase in free volume and a lower modulus. No experimental evidence of this assumption was made. On the other hand, we studied the influence of the effect of crosslinks on the storage shear modulus at room temperature: The vitrous modulus follows ob-

Table IV Static Mechanical Properties of DGEBA–3DCM Networks at 20°C

Network	T_g (°C)	x (%)	E_v (Gpa)	K_{Ic} (MPa $\sqrt{\text{m}}$)	G_{Ic} (J/m ²)	σ_y (MPa)	ϵ_y (%)
75	88	80	2.9	0.98	266	102	6.4
100	116	87	2.7	0.8	205	108	9.0
120	135	91	2.3	0.7	190	110	11.3
140	142	93	2.3	0.71	192	105	10.0
75/190	183	100	2.4	0.78	220 ^a	107	5.9
100/190	187	100	2.3	0.73	201 ^a	103	6.0
120/190	188	100	2.4	0.75	208 ^a	106	5.2
140/190	183	100	2.4	0.75	205 ^a		

^a Fragile, instable, and "stick-slip" phenomenon.

viously the same evolution—the antiplasticization phenomenon noted by Won et al.³⁰

We note a particular point at which the modulus ratio increases in the form of a step function whereas Young's modulus decreases following a step function. This special point is situated between 0.85 and 0.90 of conversion. A second effect is that at $x > 0.9$ the modulus and the β relaxation do not change. Miller and Macosko³⁶ studied theoretically the crosslink density or concentration of effective junction points in an infinite network. An effective crosslinking point is an A_f molecule, of functionality $f > 2$, with three or more branches going to infinity. For an epoxy amine system, in the case of an $A_2 + A_4$ copolymerization the probability that an A monomer will be an effective crosslink of degree 3 is given by Figure 7.³⁷ When x reaches 0.86–0.87, the probability of an amine of functionality 4 to have three branches going to infinity exactly is at its maximum. It is a special step in the statistical build-up of the network. At this point, the effective crosslinks of degree 4 are in very few number. The shape of the curve E_v vs. x probably reflects the structure of the network at this value of conversion.

On the other hand, the linear elastic fracture mechanics (LEFM) properties do not show the same variation. Figure 8, representing the variation in K_{Ic} and G_{Ic} vs. x , shows that the values decrease continuously, then increase for high degrees of conversion, $x > 0.92$, in the form of a parabolic function. The increase in K_{Ic} and G_{Ic} occurs when the effective crosslinks with four branches are statistically in larger number than the branches of degree 3. LEFM measurements show two specific behaviors before and after this point:

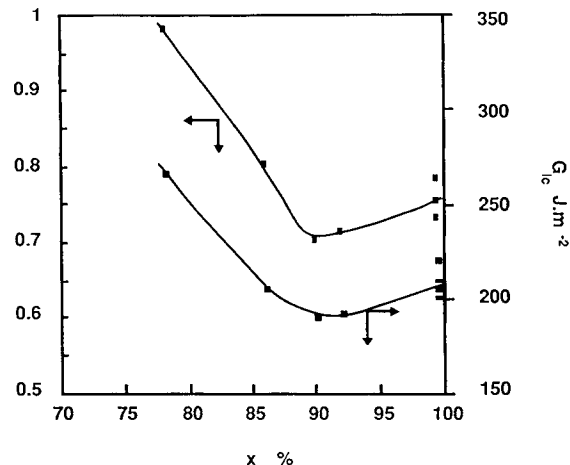


Figure 8 Critical stress intensity factor K_{Ic} and critical strain energy release G_{Ic} vs. x .

1. the crack propagation is continuous and unstable for lightly crosslinked networks
2. whereas the high T_g specimens exhibit a discontinuous and unstable crack propagation behavior called “stick-slip.”

The LEFM properties are in good agreement with the Charpy impact resistance measured by Noordam et al.¹⁰ on the same system in the same range of conversion: between 0.70 and 0.90, K_{Ic} , G_{Ic} , and the impact resistance decrease with increasing x . After $x = 0.90$, we assume that the apparition of the effective crosslinks of degree 4 may be responsible for the increase in K_{Ic} and G_{Ic} and for the changes in the propagation of the crack.

K_{Ic} is also strongly dependent upon the cure schedule or extent of reaction (Fig. 8). It is interesting to correlate the K_{Ic} variation vs. x with the shear yielding behavior. The compressive yield stress σ_y and yield strain ϵ_y increase slightly with increasing the degree of cure, whereas K_{Ic} varies on the opposite (see Table III). Yamini and Young^{37,38} have shown with an epoxy amine system that K_{Ic} decreases with increasing yield stress σ_y . A low yield stress will allow the sample to deform plastically at the crack tip, leading to the blunting of the crack and thus to an increase in the crack tip radius. It is established that the critical stress σ_c depends upon the crack tip radius: The former increases as the latter increases. K_{Ic} , which is proportional to σ_c [see eq. (10)], increases with increasing σ_c or with decreasing σ_y .

A large review of literature shows that toughness is often related to the β relaxation and low-temperature dynamical mechanical properties. Obviously, the variation in K_{Ic} and in amplitude of the β relax-

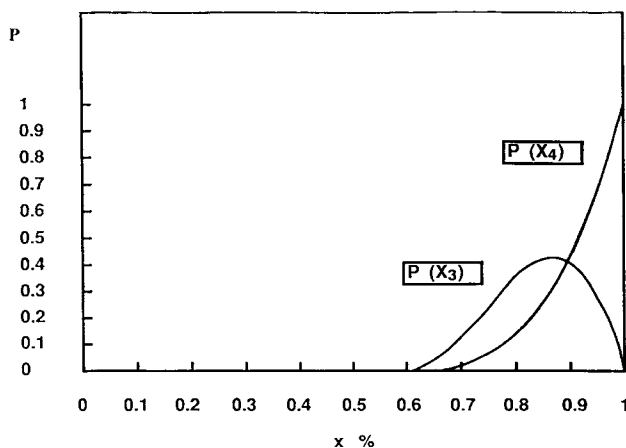


Figure 7 Probability of an A_4 monomer to have reacted three times, $P(X_3)$, and four times, $P(X_4)$, as a function of the extent of reaction.

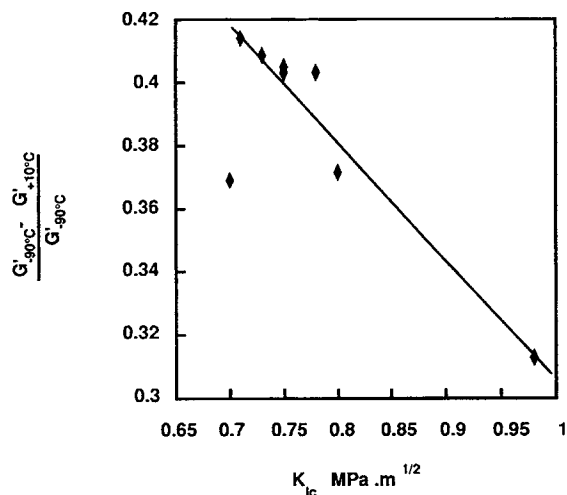


Figure 9 Magnitude of the β relaxation as a function of the critical stress intensity factor.

ation both basically depend upon the epoxy conversion. However, K_{Ic} is a macroscopic measurement representative of the ability of the material to resist to rupture. K_{Ic} is more dependent upon the molecular weight between crosslinks than on the extent of reaction itself even if the two parameters are related to each other. Thus, it seems hazardous to attribute the variation in K_{Ic} to microscopic molecular mobility, which is dependent upon x with the intermediate of the apparition of hydroxyether during the reaction. Nevertheless, we plotted the modulus ratio $G'_{-90^\circ\text{C}} - G'_{+10^\circ\text{C}} / G'_{-90^\circ\text{C}}$ as a function of K_{Ic} (see Fig. 9). The curve would testify to a sharp correlation between the two properties if we could explain sensibly the particular behavior of the 120 network, which is largely out of the curve.

CONCLUSION

This study shows that the degree of conversion can be obtained for highly crosslinked networks by determining the glass transition temperature and using the DiBenedetto equation, developed by Pascault and Williams,¹⁴ in the way used by Hale et al.¹⁶ The interest of this equation lies in the fact that no adjustable parameter is used nor statistical calculations assuming a particular model for the epoxy network build-up. Thus, the epoxy conversion can be calculated when the SEC and FTIR methods get to their limit of application.

It was shown that the extent of reaction indirectly modifies the β relaxation. In fact, it is the hydroxyether moieties appearing during the reaction that

are responsible for the changes of mobility in the network at low temperatures.

The viscoelastic behavior, at low temperatures, induces the room temperature mechanical properties such as Young's modulus, which decreases with increasing x or T_g . The apparition of effective crosslinks of degree 3 was shown to be a valuable parameter of the network to describe the variation in dynamic and tensile modulus.

The fracture properties seem to be more dependent upon the apparition of the effective crosslinks of degree 4. It does not seem reasonable to correlate the molecular mobility data to the fracture behavior because they depend upon each other through the medium of other parameters, such as crosslink density and molecular weight between crosslinks, which both depend upon the degree of conversion in this case.

The compressive behavior is in good agreement with the variation in K_{Ic} and with the results depicted in the literature.

It has been shown that precure temperature schedules do not influence the networks on the level of the mechanical properties. The quantities on the molecular scale are also considered equal within the uncertainty of determination. The only sensitive parameter to the precure temperature is the loss factor. A shoulder appears below the principal mechanical relaxation for the two networks precured at 75 and 100°C. The changes of mobility at high temperatures has not been attributed, but it is sure in the case of DGEBA-3DCM that it is not the result of secondary reactions such as etherification.

This study takes place in a larger project that includes the influence of a precure stage by microwave energy and the influence of the heating rate upon the network structure. This work will provide a comparison between the thermal and microwave precure stages on networks of equal extents of reaction.

This research was supported by the Centre National de la Recherche Scientifique, Agence Française pour la Maîtrise de l'Énergie, Electricité de France, Peugeot Société Anonyme, and the Régie Nationale des Usines Renault. The authors express their appreciation for this financial support.

REFERENCES

1. S. C. Misra, J. A. Manson, and L. H. Sperling, in *Resin Chemistry*, ACS Advances in Chemistry Series, American Chemical Society, Washington, DC, 1979, pp. 137-156.

2. J. D. LeMay, B. J. Swetlin, and F. N. Kelley, *ACS Adv. Chem. Ser.*, **243**, 165 (1984).
3. J. M. Charlesworth, *Polym. Eng. Sci.*, **28**(4), 221 (1988).
4. J. M. Charlesworth, *Polym. Eng. Sci.*, **28**(4), 230 (1988).
5. Y. G. Won, J. Galy, J. F. Gerard, and J. P. Pascault, *J. Polym. Sci.*, to appear.
6. L. E. Nielsen, *J. Macromol. Sci. Rev. Macromol. Chem.*, **C3**(1), 69 (1989).
7. T. M. Murayama and J. P. Bell, *J. Polym. Sci.*, **A2**(8), 437 (1970).
8. R. J. Morgan, F. M. Kong, and C. M. Walkup, *Polymer*, **25**, 375 (1984).
9. V. B. Gupta, L. T. Drzal, C. Y. C. Lee and M. J. Rich, *J. Macromol. Sci.-Phys.*, **B23**(4-6), 435 (1984-85).
10. A. Noordam, J. J. M. H. Wintraecken, and G. Walton, in *Crosslinked Epoxies*, B. Sedlacek and J. Kahovec, Eds., W. de Gruyter & Co, Berlin, 1987.
11. P. J. Flory, *J. Am. Chem. Soc.*, **63**, 3083 (1941).
12. W. H. Stockmayer, *J. Chem. Phys.*, **11**, 45 (1943).
13. W. H. Carothers, *Trans. Faraday Soc.*, **32**, 39 (1936).
14. J. P. Pascault and R. J. J. Williams, *J. Polym. Sci. Polym. Phys.*, **28**, 85 (1990).
15. D. Verchère, H. Sautereau, J. P. Pascault, C. C. Riccardi, S. M. Moschiar, and R. J. J. Williams, *Macromolecules*, **23**, 725 (1990).
16. A. Hale, C. W. Macosko, and H. E. Bair, *Macromolecules*, **24**, 2610 (1991).
17. P. R. Couchman, *Macromolecules*, **20**, 1712 (1987).
18. E. F. Oleinik, *Pure Appl. Chem.*, **53**, 1567 (1981); *Adv. Polym. Sci.*, **80**, 49 (1986).
19. K. Dusek, M. Clavsky, and S. Lunak, *J. Polym. Sci. Polym. Symp. Ed.*, **53**, 29 (1975).
20. K. Dusek, *Adv. Polym. Sci.*, **78**, 1 (1986).
21. A. Serier, J. P. Pascault, and T. M. Lam, *J. Polym. Sci. Polym. Chem.*, **29**, 209 (1991).
22. M. L. Williams, R. F. Landel, and J. D. Ferry, *J. Am. Chem. Soc.*, **17**, 3701 (1955).
23. J. F. Gerard, J. Galy, J. P. Pascault, J. P. Cukierman, and J. L. Halary, *Polym. Eng. Sci.*, April (1991).
24. A. K. Doolittle and D. B. Doolittle, *J. Appl. Phys.*, **28**, 901 (1957).
25. J. G. Williams, in *Fracture Mechanics of Polymers*, Ellis Horwood Ltd., Chichester, 1981, p. 292.
26. J. B. Enns and J. K. Gillham, *J. Appl. Polym. Sci.*, **28**, 2831 (1983).
27. V. B. Gupta and C. Brahathee Swaran, *J. Appl. Polym. Sci.*, **41**, 2533 (1990).
28. V. Bellenger, W. Dhaoui, and J. Verdu, *J. Polym. Sci.*, **33**, 2647 (1987).
29. Y. G. Won, J. Galy, J. P. Pascault, and J. Verdu, *Polymer*, **32**, 79 (1991).
30. Y. G. Won, J. Galy, J. F. Gerard, J. P. Pascault, V. Bellenger, and J. Verdu, *Polymer*, **31**, 1787 (1990).
31. T. Takahama and P. H. Geil, *J. Polym. Sci., Polym. Phys. Ed.*, **20**, 1979 (1982).
32. J. C. Patterson-Jones and D. A. Smith, *Appl. Polym. Sci.*, **12**, 1601 (1968).
33. R. G. C. Arridge and J. H. Speake, *Polymer*, **13**, 433 (1979).
34. J. D. Ferry, in *Viscoelastic Properties of Polymers*, John Wiley, New York, 1980, chap. 11.
35. P. Perret, Thesis 88 549, University Claude Bernard, Lyon, France, 1988.
36. D. R. Miller and C. W. Macosko, *Macromolecules*, **9**, 206 (1976).
37. S. Yamini and R. J. Young, *J. Mater. Sci.*, **15**, 1823 (1980).
38. A. J. Kinloch and R. J. Young, in *Fracture Behaviour of Polymers*, Applied Science Publishers, London, 1983, p. 4.

Received September 30, 1991

Accepted December 9, 1991